A study of stochastic FEM method for porous media flow problem

R. Blaheta
Institute of Geonics of the CAS, Ostrava, Czech Republic

M. Béreš & S. Domesová
VŠB - Technical University of Ostrava, Ostrava - Poruba, Czech Republic
Institute of Geonics of the CAS, Ostrava, Czech Republic

ABSTRACT: The paper provides an overview of the stochastic finite element method (FEM) for the investigation of the flow in heterogeneous porous materials with a microstructure being a Gaussian random field. Quantities characterizing the flow are random variables and the aim is to estimate their probability distribution. The integral mean of the velocity over the domain is one of these quantities, which is numerically analyzed for a described model problem. The estimation of those quantities is realized using the standard Monte Carlo method and the multilevel Monte Carlo method. The paper also concerns the use of the mixed finite element method for the solution of the the Darcy flow and efficient assembling and solving of the arising linear systems.

1 INTRODUCTION

Many natural materials, like geomaterials and biomaterials, possess a high level of heterogeneity which has to be properly treated for understanding and reliable modelling of processes in these materials. As a special case, we shall consider groundwater flow, which is important in many applications, as e.g. filtration and waste isolation. The groundwater flow can be further completed by transport of chemicals and pollutants or connected with deformation of the porous matrix.

The groundwater flow can be described by the boundary value problem

$$\begin{aligned} -\mathrm{div}(k\,\nabla p) &= 0 \quad \text{in } \Omega \\ p &= \widehat{p} \quad \text{on } \Gamma_D \\ (-k\,\nabla p)\cdot n &= 0 \quad \text{on } \Gamma_N, \end{aligned} \tag{1}$$

where p is the pore (water) pressure, k is permeability, $u = -k\,\nabla p$ is the Darcy's velocity, $\hat{p}$ is a given Dirichlet type boundary condition on $\Gamma_D \subset \partial\Omega$ and no flow is assumed as the Neumann type boundary condition on $\Gamma_D \subset \partial\Omega$, n is the unit outer normal to $\partial\Omega$.

We shall consider a two field form of the above boundary value problem with two basic variables $p : \Omega \to R^1$ and $u : \Omega \to R^n$

$$\begin{aligned} k^{-1}u + \nabla p &= g \\ \mathrm{div}(u) &= f \end{aligned} \Big\} \quad \text{in } \Omega$$
$$\begin{aligned} p &= \widehat{p} \quad \text{on } \Gamma_D \\ u\cdot n = u_n &= 0 \quad \text{on } \Gamma_N. \end{aligned} \tag{2}$$

We will assume that $k = k(x,\omega)$ is a random variable, $x \in \Omega$ and $\omega \in S$. Here S is a sample space equipped by a suitable probability model with given parameters. Then the model outputs as p, u and another quantities $J(p,\, u)$, e.g. the averages

$$\langle \nabla p \rangle = \frac{1}{|\Omega|}\int_\Omega \nabla p \tag{3}$$

and

$$\langle u \rangle = \frac{1}{|\Omega|}\int_\Omega -k\nabla p u \tag{4}$$

will be also random variables and we will be interested in their characteristics as the mean (expectation) $\mathbb{E}$ and variance $\mathbb{V}$.

2 STOCHASTIC MICROSTRUCTURE

The permeability $k = k(x,\omega)$ can be considered as a random field in the domain Ω or in selected points within Ω. Especially, we shall assume that

$$\ln(k(x,\cdot)) = c_1\phi,\ \ \phi \in N(\mu,\sigma^2), \tag{5}$$

where $N(\mu,\sigma^2)$ denote the normal distribution with the mean μ and variance σ^2. This lognormal character of permeability is supported by experimental tests on rock as well as experimentally found logarithmic relation between permeability and porosity, see (Nelson

et al. 1994, Freeze 1975). Thus ϕ in (5) could be interpreted as the porosity which gives to (5) a physical meaning.

If $X \in R^n$ is a random field, such that $X_i \in N(0,1)$, then the random field k connected with selected points $x^{(i)} \in \Omega,\ i = 1, \ldots, n$, can be generated as

$$\ln(k) = c_1(\sigma X + \mu), \tag{6}$$

i.e. $k = e^{c_1\mu} e^{c_1\sigma X}$. For numerical experiments we shall use $c_1 = 1$, $\mu = 0$, i.e.

$$k = e^{\sigma X}. \tag{7}$$

In this case the components of k have lognormal distribution with the mean $e^{\sigma^2/2}$ and variance $\left(e^{\sigma^2} - 1\right) e^{\sigma^2}$.

The random field X can be further smoothed by correlation, which provides the correlated random field X^c. The correlation is frequently described as an exponential expression involving a correlation length λ, e.g.

$$\begin{aligned} c(x,\, y) &= c(X^c(x), X^c(y)) \\ &= \sigma^2 exp\left(-\left\|x - y\right\| / \lambda\right). \end{aligned} \tag{8}$$

Different methods can be used to generate the correlated random field. The Choleski factorization of the correlation matrix C is probably the most straightforward one and will be used within the experiments in this paper. Further methods as a technique based on the discrete Fourier transform can be found in the literature, see e.g. (Lord, Powell, & Shardlow 2014, Powell 2014).

Given the set of selected points $x^{(i)} \in \Omega,\ i = 1, \ldots, n$, we can define the correlation matrix C by

$$\begin{aligned} C &= \mathbb{E}((X - \mathbb{E}(X))(X - \mathbb{E}(X))^T) = \\ &= \mathbb{E}(XX^T) - \mathbb{E}(X)\mathbb{E}(X^T) \end{aligned} \tag{9}$$

In the case of $\mathbb{E}(X) = 0$, it provides

$$C = \mathbb{E}(XX^T),\ C_{ij} = c(x^{(i)},\, x^{(j)}). \tag{10}$$

Theorem 1. *(Generation of the correlated random field). Let $C = LL^T$ be the Choleski factorization of C, X be an uncorrelated random field, $X_i \in N(0,1)$. Then $X^c = LX$ is the correlated random field with correlation matrix C. We can write $X^c \in N(0, C)$.*

Proof. If X_i are uncorrelated and have zero mean and unit variance for any i, then $\mathbb{E}(X_i X_j) = \delta_{ij}$ and therefore $\mathbb{E}(XX^T) = I$. The correlation matrix is SPD and therefore the Choleski factorization exists. For $X^c = LX$, where L is the Choleski factor, it holds

$$\begin{aligned} \mathbb{E}(X^c(X^c)^T) &= \mathbb{E}(LXX^TL^T) \\ &= L\mathbb{E}(XX^T)L^T \\ &= LL^T = C \end{aligned} \tag{11}$$

Note that the identity $\mathbb{E}(LXX^TL^T) = L\mathbb{E}(XX^T)L^T$ follows from the linearity of the expectation operator $\mathbb{E}$. □

2.1 *Model problem*

As a model problem, we shall consider the groundwater flow given by equation (1) on the unit square $\Omega = \langle 0,\, 1\rangle \times \langle 0,\, 1\rangle$ with the specific boundary conditions - the pressure difference in x_1 direction, see Figure 1.

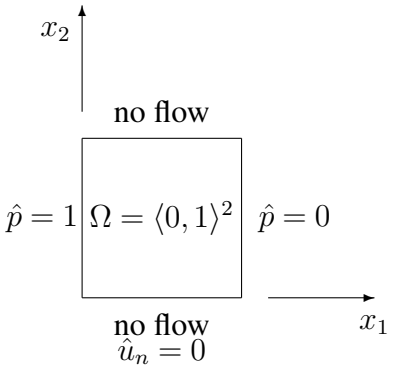

Figure 1: Test problem with pressure difference in x_1 direction

We shall be interested in different quantities as e.g.

- $u(0.5,\, 0.5)$,
- $k_{eff} = \int_0^1 u(1,\, x_2) dx_2$,
- $\langle u \rangle = \frac{1}{|\Omega|} \int_\Omega u = \frac{-1}{|\Omega|} \int_\Omega k \nabla p^{(i)}$.

For the realization of this calculations the mixed FEM method can be used, see section 4. If the permeability k will be a random field in Ω, then these quantities will be also random variables and we shall compute their characteristics like the expectation and variance.

2.2 *Visualization of the generated fields*

For numerical experiments with the model problem, we use different values $\sigma \in \{1,\, 2,\, 4\}$ and $\lambda \in \{0.3,\, 0.1\}$.

The following figures show the visualization of the generated random field k for six combinations of parameters σ and λ value. All of the Gaussian random fields were created from the same random vector X, where $X_i \sim N(0,1)$, so we can observe the effect of the parameters σ and λ changes on the material microstructure.

The Figures 2, 3, 4, 5, 6, 7 show that the changes of the parameter σ affects only the logarithmic scale of the values, which is caused by the linear relation between $\log k$ and σ^2. The influence of the parameter λ can be observed in a smoother material with growing λ.

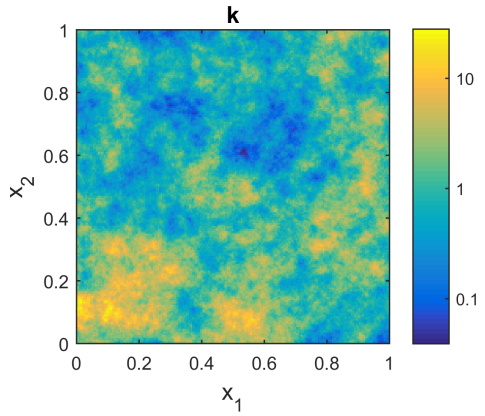

Figure 2: Random field for parameters: $\sigma = 1$, $\lambda = 0.1$

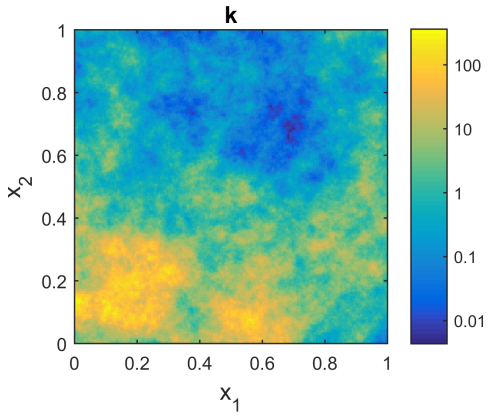

Figure 6: Random field for parameters: $\sigma = 2$, $\lambda = 0.3$

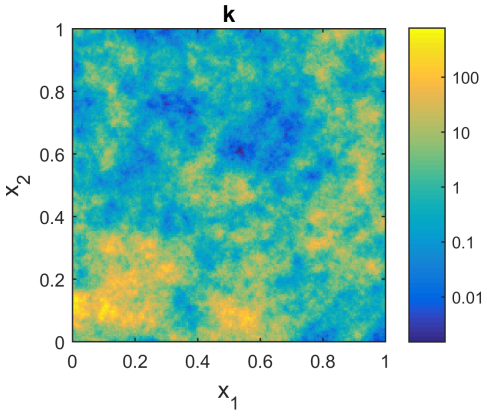

Figure 3: Random field for parameters: $\sigma = 2$, $\lambda = 0.1$

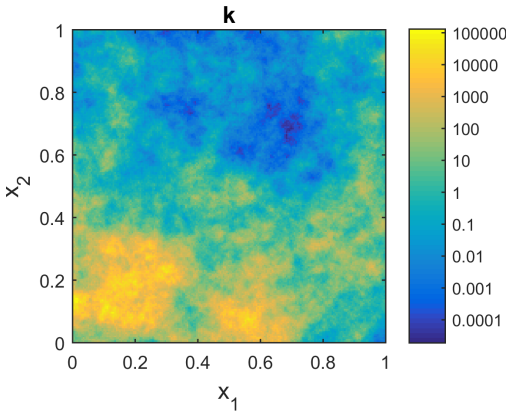

Figure 7: Random field for parameters: $\sigma = 4$, $\lambda = 0.3$

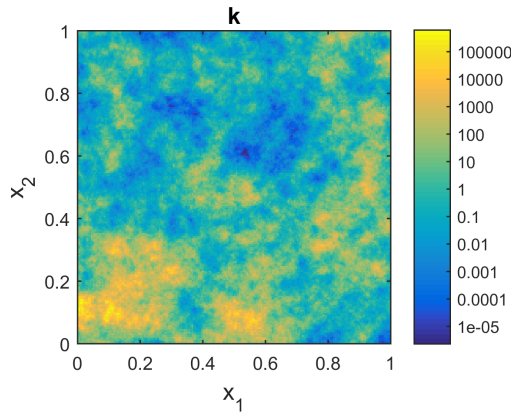

Figure 4: Random field for parameters: $\sigma = 4$, $\lambda = 0.1$

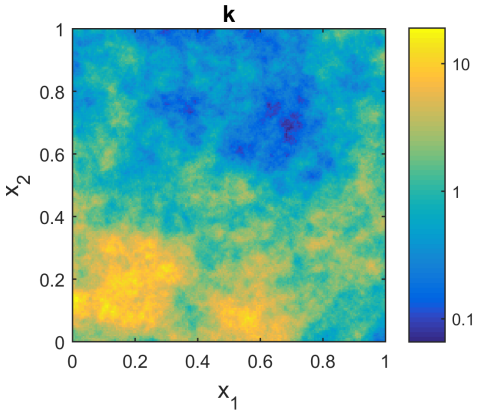

Figure 5: Random field for parameters: $\sigma = 1$, $\lambda = 0.3$

3 MONTE CARLO METHODS

Consider the Darcy flow model problem. We are interested in the estimation of the quantities

$$u(0.5, 0.5), \; k_{eff} \text{ and } \langle u \rangle . \tag{12}$$

In the case of the Monte Carlo (MC) simulations, we consider this quantities as random variables.

3.1 *Standard Monte Carlo method*

Using the standard MC method, the expectation $\mathbb{E}(\phi)$ of a random variable ϕ is estimated as a sample average

$$\frac{1}{N} \sum_{n=1}^{N} \phi^{(n)}, \tag{13}$$

where $\phi^{(n)}$ for $n \in \{1, \ldots, N\}$ are random samples of ϕ. The estimated probability distribution of the random variables is also described by the sample standard deviation, the estimated probability density function (pdf) and cumulative distribution function (cdf).

The variance of the MC estimator is calculated as

$$V_{MC} = \frac{1}{N} s^2, \tag{14}$$

where s is the sample standard deviation.

The experiments were performed with the following parameters: grid size: 200×200, $\sigma \in \{1, 2, 4\}$, $\lambda \in \{0.1, 0.3\}$, number of experiments: $2 \cdot 10^4$.

The following tables show the estimated sample average and sample standard deviation for the random variables $u_{x_1}(0.5,\, 0.5)$, $u_{x_2}(0.5,\, 0.5)$, $\langle u \rangle_{x_1}$ and $\langle u \rangle_{x_2}$. The values after the $\pm$ symbol correspond to the 95% confidence interval for the estimated value. For the random variable k_{eff} the same estimation as for $\langle u \rangle_{x_1}$ was obtained. The graphs in Figure 8 show the pdf and cdf estimation for the random variable $\langle u \rangle_{x_1}$.

Table 1: Sample average of $u_{x_1}(0.5,\, 0.5)$

	$\lambda = 0.3$	$\lambda = 0.1$
$\sigma = 1$	1.135 ± 0.0132	1.0409 ± 0.0096
$\sigma = 2$	1.7244 ± 0.055	1.1649 ± 0.0251
$\sigma = 4$	11.9402 ± 1.8383	1.9334 ± 0.1447

Table 2: Sample standard deviation of $u_{x_1}(0.5,\, 0.5)$

	$\lambda = 0.3$	$\lambda = 0.1$
$\sigma = 1$	0.9504 ± 0.0093	0.6902 ± 0.0068
$\sigma = 2$	3.9656 ± 0.0389	1.8104 ± 0.0177
$\sigma = 4$	132.6336 ± 1.2999	10.4422 ± 0.1023

Table 3: Sample average of $u_{x_2}(0.5,\, 0.5)$

	$\lambda = 0.3$	$\lambda = 0.1$
$\sigma = 1$	0.0008 ± 0.0062	-0.0006 ± 0.0058
$\sigma = 2$	-0.0276 ± 0.03	0.002 ± 0.0169
$\sigma = 4$	0.512 ± 1.1175	0.0173 ± 0.0968

Table 4: Sample standard deviation of $u_{x_2}(0.5,\, 0.5)$

	$\lambda = 0.3$	$\lambda = 0.1$
$\sigma = 1$	0.4492 ± 0.0044	0.4201 ± 0.0041
$\sigma = 2$	2.1625 ± 0.0212	1.2215 ± 0.012
$\sigma = 4$	80.627 ± 0.7902	6.9851 ± 0.0685

Table 5: Sample average of $\langle u \rangle_{x_1}$

	$\lambda = 0.3$	$\lambda = 0.1$
$\sigma = 1$	1.1228 ± 0.0083	1.018 ± 0.0032
$\sigma = 2$	1.6821 ± 0.0324	1.0983 ± 0.0079
$\sigma = 4$	10.0822 ± 0.9339	1.7447 ± 0.0409

Table 6: Sample standard deviation of $\langle u \rangle_{x_1}$

	$\lambda = 0.3$	$\lambda = 0.1$
$\sigma = 1$	0.6024 ± 0.0059	0.2335 ± 0.0023
$\sigma = 2$	2.34 ± 0.0229	0.5695 ± 0.0056
$\sigma = 4$	67.3806 ± 0.6604	2.9495 ± 0.0289

Table 7: Sample average of $\langle u \rangle_{x_2}$

	$\lambda = 0.3$	$\lambda = 0.1$
$\sigma = 1$	0.0005 ± 0.0015	0.0001 ± 0.001
$\sigma = 2$	-0.003 ± 0.0062	-0.0002 ± 0.0022
$\sigma = 4$	-0.02 ± 0.1623	-0.0023 ± 0.0109

Table 8: Sample standard deviation of $\langle u \rangle_{x_2}$

	$\lambda = 0.3$	$\lambda = 0.1$
$\sigma = 1$	0.1098 ± 0.0011	0.069 ± 0.0007
$\sigma = 2$	0.4499 ± 0.0044	0.1596 ± 0.0016
$\sigma = 4$	11.7075 ± 0.1147	0.7865 ± 0.0077

3.2 *Multilevel Monte Carlo method*

For the mean value $\mathbb{E}(\phi_L)$ of a random variable $\phi = \phi_L$ we can write

$$\mathbb{E}(\phi_L) = \mathbb{E}(\phi_0) + \sum_{l=1}^{L} \mathbb{E}(\phi_l - \phi_{l-1}). \tag{15}$$

This leads to the multilevel Monte Carlo (MLMC) estimator

$$\mathbb{E}(\phi_L) \approx \frac{1}{N_0} \sum_{n=1}^{N_0} \phi_0^{(n)} + \sum_{l=1}^{L} \frac{1}{N_l} \sum_{n=1}^{N_l} \left(\phi_l^{(n)} - \phi_{l-1}^{(n)} \right), \tag{16}$$

see (Cliffe, Giles, Scheichl, & Teckentrup 2011, Barth, Schwab, & Zollinger 2011). For different levels $l \in \{1, \ldots, L\}$ the values $\phi_l^{(n)} - \phi_{l-1}^{(n)}$ are independent. However the values $\phi_l^{(n)}$ and $\phi_{l-1}^{(n)}$ for specific $n \in \{1, \ldots, N\}$ are correlated.

The variance of the MLMC estimator can be calculated as

$$V_{MLMC} = \sum_{l=0}^{L} \frac{1}{N_l} s_l^2, \tag{17}$$

where s_l is the sample standard deviation on the level l.

This approach was applied to the model problem with the grid size $d \times d$. We were interested in the random variable $\phi = \phi_L = \langle u \rangle_{x_1}^{(d)}$, i.e. the integral mean of the velocity over the $\langle 0, 1 \rangle \times \langle 0, 1 \rangle$ domain calculated for the grid size $d \times d$. Samples of the random variable $\phi_{L-1} = \langle u \rangle_{x_1}^{(d/2)}$ are calculated as the integral mean of the velocity for the grid $\frac{d}{2} \times \frac{d}{2}$, etc.

There are different ways of calculating the coarse grid approximation ϕ_{l-1} of ϕ_l in order to achieve strong correlation between this two random variables (high correlation between ϕ_{l-1} and ϕ_l leads to low variance on the MLMC level l). In this paper we describe two possible procedures for the coarse grid approximation.

Procedure 1: Coarse grid approximation preserving the Gaussian random field distribution

The samples $\phi_l^{(n)}$ and $\phi_{l-1}^{(n)}$ should be correlated, therefore it is necessary to determine the way of $\phi_{l-1}^{(n)}$ calculation. The value of $\phi_l^{(n)}$ corresponds to a specific sample $k^{(d)}$ of the Gaussian random field, which was

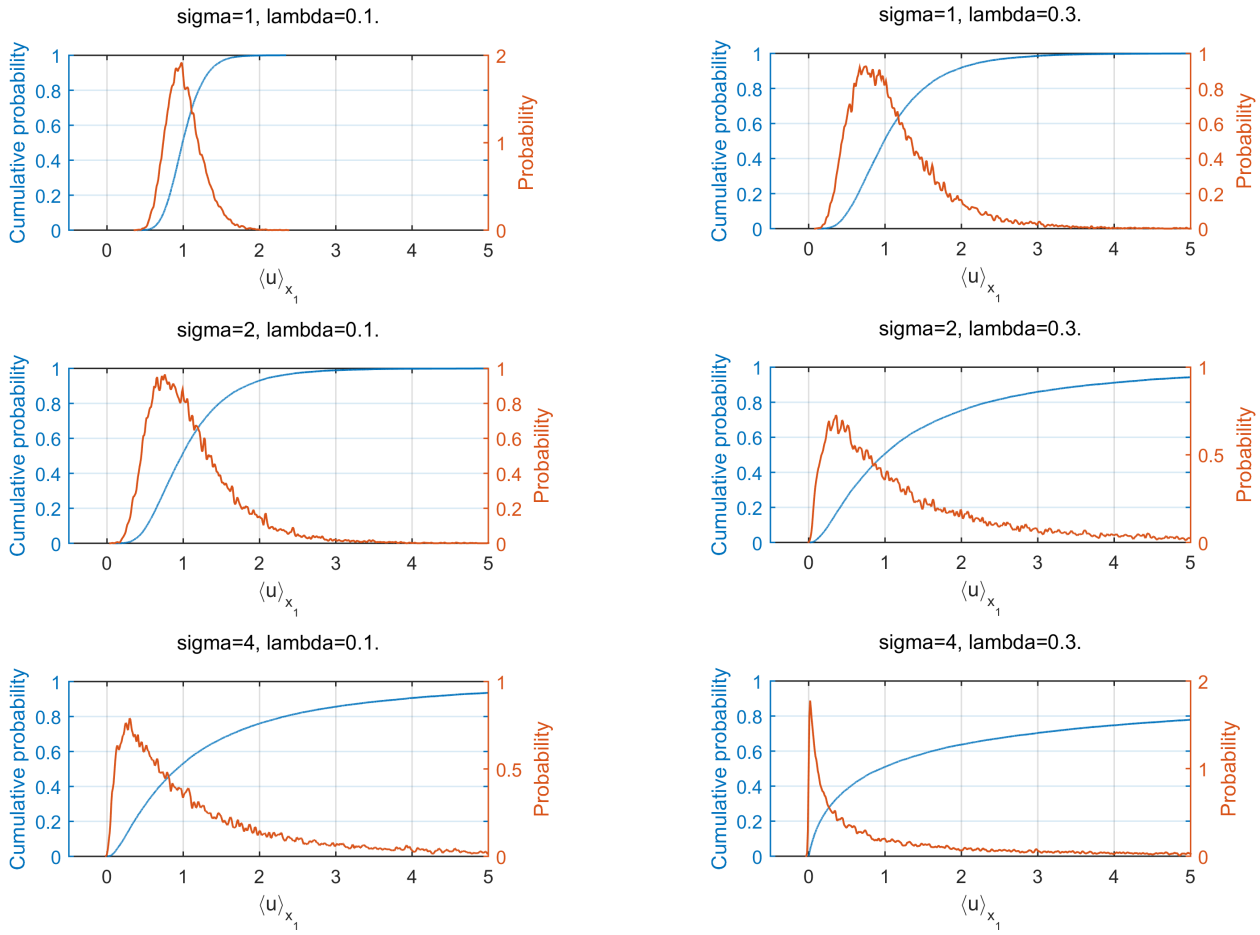

Figure 8: Estimated pdf and cdf of $\langle u \rangle_{x_1}$ for $\lambda = 0.1$ (left) and $\lambda = 0.1$ (right)

obtained for a random vector X, where $X_i \sim N(0,1)$, $i \in \{1, \ldots, d^2\}$. To obtain the value $\phi_{l-1}^{(n)}$ we first create a coarse material $k^{(d/2)}$ from a vector Y of length $\frac{1}{4}d^2$, which is calculated from the vector X values. For example

$$Y_1 = \frac{1}{2}(X_1 + X_2 + X_{d+1} + X_{d+2}) \tag{18}$$

(weighted arithmetic mean), etc. This approach ensures that the values Y_i follow the $N(0,1)$ distribution, therefore the obtained material $k^{(d/2)}$ is also a Gaussian random field. The value of $\phi_{l-1}^{(n)}$ is then calculated on the coarse grid and remains correlated with the value of $\phi_l^{(n)}$.

The MLMC method was tested on the model problem with grid size 200×200, therefore is was possible to use three coarser grids of dimensions 100×100, 50×50 and 25×25. The numbers of samples N_l to be performed on specific levels were calculated from a preliminary simulation run. In this run the same number of samples was performed on each level and then the values of computation time T_l and sample standard deviation s_l were estimated for each level. The values of N_l were then calculated according to (Cliffe, Giles, Scheichl, & Teckentrup 2011) as $N \cdot \sqrt{\frac{s_l^2}{T_l}}$, where N is a constant common to all the levels.

The table 9 presents the results of the MLMC method that can be compared with the MC method results (table 5).

Table 9: MLMC method results for $\langle u \rangle_{x_1}$

	$\lambda = 0.3$	$\lambda = 0.1$
$\sigma = 1$	1.1302 ± 0.0039	1.0189 ± 0.0007
$\sigma = 2$	1.6744 ± 0.0189	1.1003 ± 0.0021
$\sigma = 4$	9.6647 ± 0.5259	1.745 ± 0.0152

The MLMC results were calculated with different number of samples (i.e. different computation time) than the MC results, therefore we propose the following indicator for comparison of the efficiency. The efficiency of the MLMC estimator in comparison to the MC estimator will be calculated as

$$\frac{V_{MC}}{V_{MLMC}} \cdot \frac{T_{MC}}{T_{MLMC}}, \tag{19}$$

where T_{MC} is the total time of the MC simulation and T_{MLMC} time of the MLMC simulation, see the table 10.

Table 10: MLMC/MC efficiency calculated via (19)

	$\lambda = 0.3$	$\lambda = 0.1$
$\sigma = 1$	1.9382	7.7148
$\sigma = 2$	1.1841	5.7974
$\sigma = 4$	1	3.0011

The value 1 for $\sigma = 4$ and $\lambda = 0.3$ in table 10 is caused by the fact that in this case it was evaluated

in the preliminary run, that only one level should be used, i.e. it is the standard MC method. In the remaining cases all of the 4 levels were used.

The table 11 shows the values of s_l^2 on each of the levels $l \in \{1, \ldots, 4\}$ calculated in the preliminary run (level $l = 1$ corresponds to the coarsest grid, while the remaining values present the difference between the fine and coarse grid on the given level). We used these values to calculate the numbers of samples to be executed on each of the MLMC levels.

Table 11: Variance on each MLMC level

σ	λ	$l = 4$	$l = 3$	$l = 2$	$l = 1$
1	0.3	$4.4{\cdot}10^{-2}$	$4.1{\cdot}10^{-2}$	$3.6{\cdot}10^{-2}$	0.35
	0.1	$1.4{\cdot}10^{-3}$	$1.2{\cdot}10^{-3}$	$1{\cdot}10^{-3}$	$5.4{\cdot}10^{-2}$
2	0.3	1.4	0.84	1	4.5
	0.1	$1.1{\cdot}10^{-2}$	$1{\cdot}10^{-2}$	$1.1{\cdot}10^{-2}$	0.29
4	0.3	$1{\cdot}10^{5}$	$5.1{\cdot}10^{3}$	$9.3{\cdot}10^{3}$	$2.3{\cdot}10^{4}$
	0.1	0.63	0.76	0.91	4.5

The following table shows the ratio of the numbers of samples, that were used on different levels.

Table 12: Ratios of N_l/N_4 values for the six combinations of parameters

σ	λ	N_4	N_3	N_2	N_1
1	0.3	1	2.23	4.70	33.86
	0.1	1	2.12	4.53	75.15
2	0.3	1	1.73	4.35	20.97
	0.1	1	2.19	5.04	60.55
4	0.3	1	-	-	-
	0.1	1	2.51	6.21	32.24

Procedure 2: Coarse grid approximation as arithmetic mean of correlated random field

In this case we use a similar approach as in the procedure 1, but the key difference is that the smoothing is applied to the correlated values,

$$Y_1^c = \frac{1}{4}\left(X_1^c + X_2^c + X_{d+1}^c + X_{d+2}^c\right) \tag{20}$$

(arithmetic mean). A disadvantage is that this coarse grid approximation is not the same random field, so in the lower MLMC levels we always need to construct a new covariance matrix and its Choleski factorization. The new covariance matrix is created by averaging of elements of the fine grid covariance matrix according to the fine grid to coarse grid elements mapping, this construction comes from the linearity of the covariance. This disadvantage is compensated by very high correlation between fine grid and coarse grid approximation.

In the figure 9 we show an example of coarse grid approximations for both procedures.

The table 13 presents the results obtained for $\langle u \rangle_{x_1}$ (including 95% confidence interval). The calculated efficiency compared to the MC estimator via formula (19) can be seen in the table 14.

Table 13: MLMC method results for $\langle u \rangle_{x_1}$

	$\lambda = 0.3$	$\lambda = 0.1$
$\sigma = 1$	1.1298 ± 0.0011	1.0189 ± 0.0004
$\sigma = 2$	1.6945 ± 0.0044	1.1001 ± 0.0012
$\sigma = 4$	10.3715 ± 0.2517	1.7434 ± 0.0087

Table 14: MLMC efficiency calculated via (19)

	$\lambda = 0.3$	$\lambda = 0.1$
$\sigma = 1$	101.2564	90.7969
$\sigma = 2$	87.3758	72.5988
$\sigma = 4$	23.1090	38.6652

The table 15 shows the values of s_l^2 on each of the levels $l \in \{1, \ldots, 4\}$ calculated in the preliminary run.

Table 15: Variance on each MLMC level

σ	λ	$l = 4$	$l = 3$	$l = 2$	$l = 1$
1	0.3	$4.4{\cdot}10^{-8}$	$1.3{\cdot}10^{-6}$	$6.2{\cdot}10^{-6}$	0.36
	0.1	$1.1{\cdot}10^{-7}$	$1.9{\cdot}10^{-6}$	$9.6{\cdot}10^{-6}$	$5.4{\cdot}10^{-2}$
2	0.3	$7.5{\cdot}10^{-6}$	$2.0{\cdot}10^{-4}$	$1.0{\cdot}10^{-3}$	5.5
	0.1	$5.1{\cdot}10^{-6}$	$9.9{\cdot}10^{-5}$	$4.1{\cdot}10^{-4}$	$3.1{\cdot}10^{-1}$
4	0.3	$1.4{\cdot}10^{-1}$	1.7	$6.2{\cdot}10^{1}$	$1.1{\cdot}10^{4}$
	0.1	$2.1{\cdot}10^{-3}$	$2.0{\cdot}10^{-2}$	$1.2{\cdot}10^{-1}$	7.2

The following table shows the ratio of the numbers of samples, that were used on different levels. In all the six cases at least three levels were used.

Table 16: Ratios of N_l/N_4 values for the six combinations of parameters

σ	λ	N_4	N_3	N_2	N_1
1	0.3	1	12.20	60.45	31410.66
	0.1	1	9.66	49.56	9127.92
2	0.3	1	11.56	47.65	10186.95
	0.1	1	9.66	47.36	2942.09
4	0.3	1	11.32	41.83	2550.90
	0.1	1	8.04	38.23	906.28

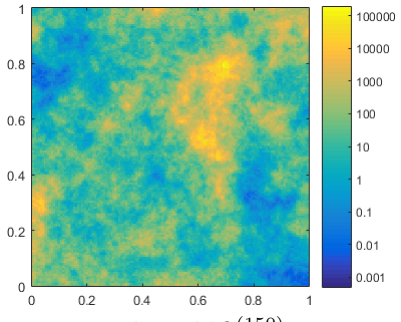

Fine grid $k^{(150)}$

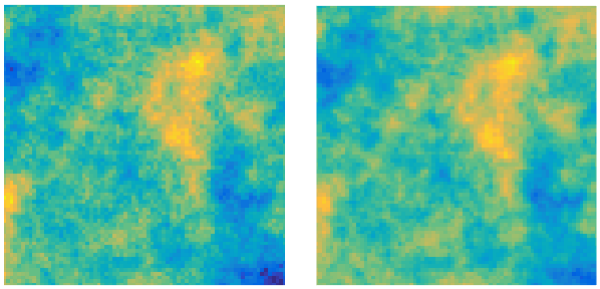

Coarse grids $k^{(75)}$ (left procedure 1; right procedure 2)

Figure 9: Comparison of coarse grid approximations

4 MIXED FEM DISCRETIZATION AND SOLUTION

The groundwater flow (1) can be implemented by the mixed finite element method, e.g. in the way described in (Cliffe, Graham, Scheichl, & Stals 2000, Blaheta, Hasal, Domesová, & Béreš 2014). The first advantage of the mixed formulation is in more accurate approximation of both pressures and velocities. The random permeability field sampling then requires repeated assembling and solving of the mixed FEM system, which has the following saddle point structure

$$\begin{array}{rcl} Mu \quad +B^T p & = & G \\ Bu & = & F \end{array} \tag{21}$$

Note that only the velocity mass matrix M depends on realization $\omega \in S$,

$$M_{ij} = M_{ij}(\omega) = \int_\Omega k(\omega)^{-1} \Phi_j \Phi_i \, d\Omega, \tag{22}$$

where Φ_j, Φ_i are basis functions in the lowest order Raviart-Thomas space. The repeated assembling of the matrix

$$\mathcal{A} = \begin{bmatrix} M & B^T \\ B & 0 \end{bmatrix} \tag{23}$$

is therefore restricted to the pivot block. A fast assembling of both M and B is implemented in the RT1 code, see (Blaheta, Hasal, Domesová, & Béreš 2014).

As a solution of the system, the discretized pressure p and velocity u is obtained. The following graphs at figures 10, 11 and 12 show the visualization of the solution for an example given by the Gaussian random field 3.

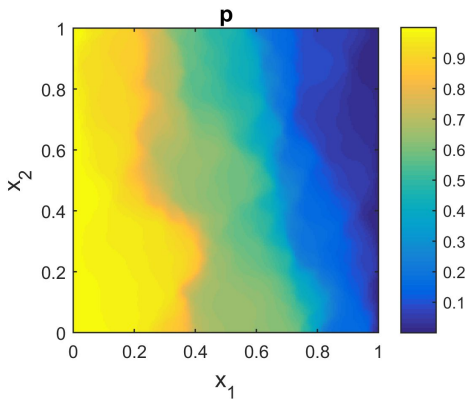

Figure 10: Discretized pressure p

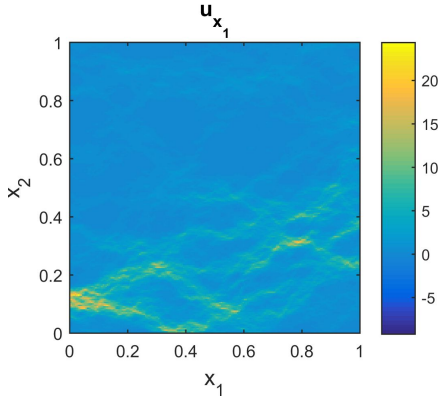

Figure 11: Discretized velocity u (first coordinate)

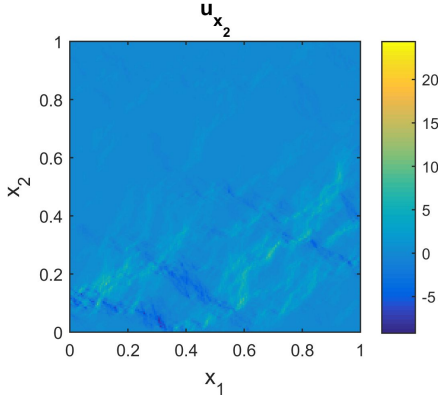

Figure 12: Discretized velocity u (second coordinate)

When repeatedly solving the system (21) by a direct method, the benefit of B not dependent on sampling is not exploited. The use of an iterative solution method, such as MINRES or GMRES, with block preconditioner, provides the chance to save some effort as only the block corresponding to M is changing. It is the case the following preconditioners

$$\mathcal{P}_1 = \begin{bmatrix} \tilde{M} + B^T W^{-1} B & \zeta B^T \\ 0 & W \end{bmatrix}, \tag{24}$$

with $\tilde{M}$ being a suitable approximation to M and W being a block independent on sampling, e.g. $W = \frac{1}{r} I$, where r is a (large) regularization parameter, $\zeta \in \{0, 1, 2\}$. Special cases are $\tilde{M}$ being a mass matrix for the mean value of the permeability k, $\tilde{M} = \frac{\text{trace}\,(M)}{\text{trace}\,(I)} I$ and $W = BB^T$, when $B^T W^{-1} B$ becomes a projection.

Other possibilities are preconditioners for the transformed system with the matrix

$$\mathcal{A}_- = \begin{bmatrix} M & B^T \\ -B & 0 \end{bmatrix} \tag{25}$$

as the HSS preconditioner

$$\mathcal{P}_2 = \begin{bmatrix} M + \alpha I & 0 \\ 0 & \alpha I \end{bmatrix} \begin{bmatrix} \alpha I & B^T \\ -B & \alpha I \end{bmatrix} \tag{26}$$

or relaxed HSS preconditioner

$$\mathcal{P}_3 = \begin{bmatrix} M & 0 \\ 0 & \alpha I \end{bmatrix} \begin{bmatrix} \alpha I & B^T \\ -B & 0 \end{bmatrix} \tag{27}$$

with a suitable parameter α.

5 CONCLUSIONS

The article presents the first results of the authors in the field of the stochastic partial differential equations (PDEs) or stochastic FEM methods. The simple and multilevel Monte Carlo methods are used as tools for stochastic simulations.

We study the mixed FEM calculation of the Darcy flow problem with stochastic material coefficients. We focused on the characterizations of the velocity, especially on the integral average of velocity over the domain and the velocity in the middle of the the domain.

The MC approach was used for the estimation of the expected value, variance and distribution of the studied random variables.

The MLMC method was used for the more efficient estimation of the expected value of the random variable $\langle u \rangle_{x_1}$. We presented two approaches to the coarse grid approximation, the first one is straightforward and preserves the Gaussian random distribution on the coarse grid, but was inefficient due to low correlation between the fine and coarse grid approximation. The second one suffers from the more difficult sample generation on the coarse grids. Nevertheless the second approach was more efficient than the first one, according to tables 10 and 14. Depending on the problem parameters λ and σ we achieved variance reduction from about $23\times$ to $101\times$.

The work is in progress, we plan to use a different approach to the Gaussian random field generation based on the Karhunen-Loève (K-L) decomposition. This will allow us to solve the problem on larger grids and as well it provides a different way of using the MLMC method (MLMC levels will correspond to the levels of the K-L decomposition). The K-L decomposition also provides a different approach to the stochastic PDEs solving by e.g. the collocation method or the stochastic Galerkin method.

ACKNOWLEDGEMENT

This work was supported by The Ministry of Education, Youth and Sports from the National Programme of Sustainability (NPU II) project „IT4Innovations excellence in science - LQ1602“.

REFERENCES

Barth, A., C. Schwab, & N. Zollinger (2011). Multi-level monte carlo finite element method for elliptic pdes with stochastic coefficients. *Numerische Mathematik 119*(1), 123–161.

Blaheta, R., M. Hasal, S. Domesová, & M. Béreš (2014). Rt1-code: A mixed rt0-p0 raviart-thomas finite element implementation. http://www.ugn.cas.cz/publish/software/RT1-code/RT1-code.zip.

Cliffe, K., M. Giles, R. Scheichl, & A. L. Teckentrup (2011). Multilevel monte carlo methods and applications to elliptic pdes with random coefficients. *Computing and Visualization in Science 14*(1), 3–15.

Cliffe, K., I. G. Graham, R. Scheichl, & L. Stals (2000). Parallel computation of flow in heterogeneous media modelled by mixed finite elements. *Journal of Computational Physics 164*(2), 258–282.

Freeze, R. A. (1975). A stochastic-conceptual analysis of one-dimensional groundwater flow in nonuniform homogeneous media. *Water Resources Research 11*(5), 725–741.

Lord, G. J., C. E. Powell, & T. Shardlow (2014). *An Introduction to Computational Stochastic PDEs*. Cambridge University Press.

Nelson, P. H. et al. (1994). Permeability-porosity relationships in sedimentary rocks. *The log analyst 35*(03), 38–62.

Powell, C. E. (2014). Generating realisations of stationary gaussian random fields by circulant embedding. https://www.nag.co.uk/doc/techrep/pdf/tr1_14.pdf.